



Proof of Concept of the Quantum Capacitance Detector

J. Bueno*, M. D. Shaw**, P. K. Day, C.M. Bradford and P. M. Echternach

Jet Propulsion Laboratory, California Institute of Technology

Electron Beam Lithography by Richard E. Muller

With many thanks to Jonas Zmuidzinis, Rick LeDuc, Per Delsing (Chalmers) and Ben Palmer (Laboratory for Physical Sciences)

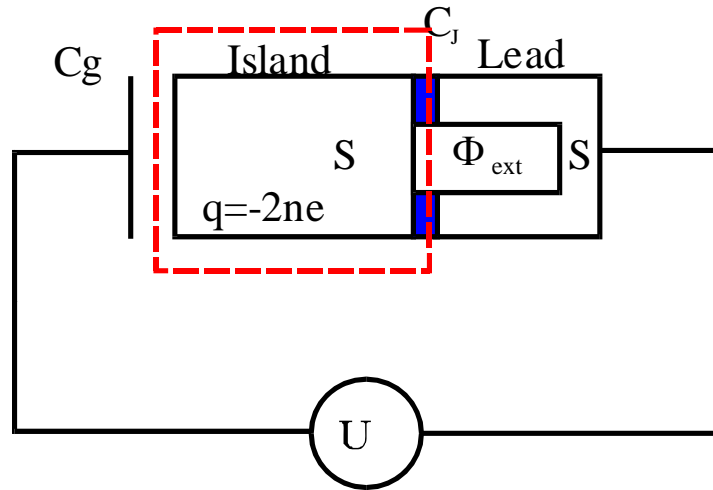
* present address: Center for Astrobiology (CSIC-INTA), Spain.

** present address: Applied Physics, California Institute of Technology

This work was performed at the Jet Propulsion Laboratory, California Institute of Technology, under a contract with the National Aeronautics and Space Administration



Single Cooper-Pair Box



Electrostatic gate charge $n_G = \frac{C_G V_G}{2e}$

Charging energy $E_C = \frac{e^2}{2C_\Sigma}$

Josephson coupling $E_J = E_J^{\max} \left| \cos \left(\frac{\pi \Phi}{\Phi_0} \right) \right|$

$$H = 4E_C \sum_n (n - n_G)^2 |n\rangle\langle n| - \frac{E_J}{2} \sum_n (|n+1\rangle\langle n| + |n\rangle\langle n+1|)$$



Energy levels, Coulomb Staircase and Quantum Capacitance

- In the absence of Josephson coupling, Energy is given by parabolas centered at integer values of Cooper Pair Charge

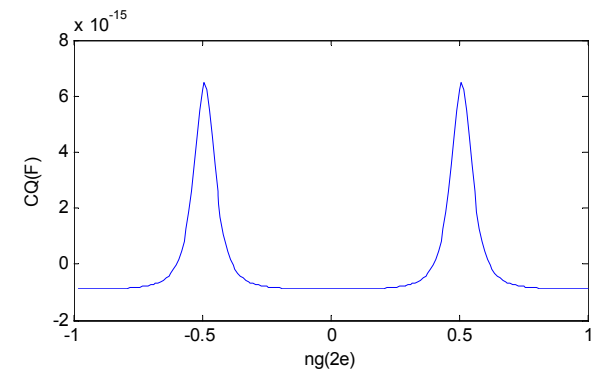
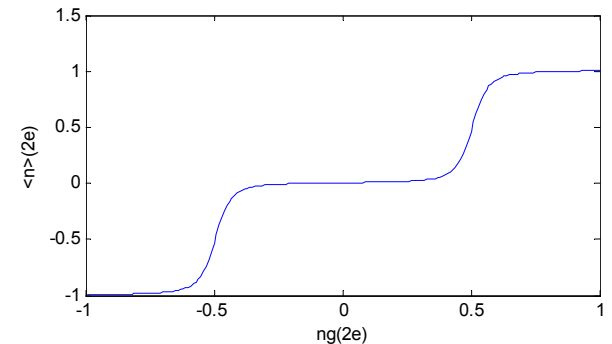
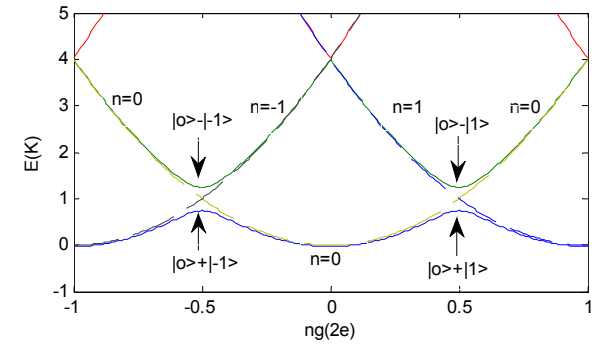
$$E = (Q - 2ne)^2 = (C_g V_g - 2ne)^2$$

- As the gate voltage is increased, Cooper Pairs tunnel to minimize the energy and the charge on the island changes in a stepwise fashion

- The capacitance of the island $C_Q = 2e \frac{d\langle n \rangle}{dV_g}$ spikes up at the

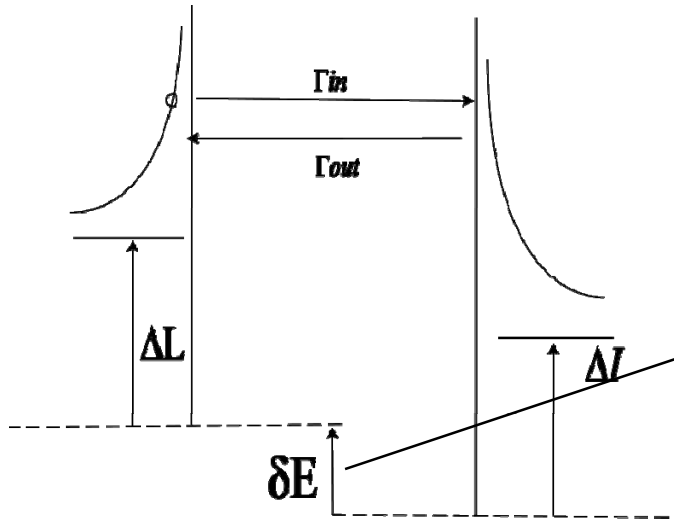
degeneracy points where the charge in the island is changing fast

- The Josephson Coupling introduces splittings in the energy levels
- Eigenvectors are symmetrical and anti-symmetrical combinations of the charge states
- The larger E_j , the “rounder” the charge staircase and the smaller the capacitance peaks
- In the absence of tunneling, only one parabola would exist ($n=0$) and the capacitance would be constant as a function of the gate voltage
- The variable capacitance is due to the quantum nature of the system and is called the quantum capacitance

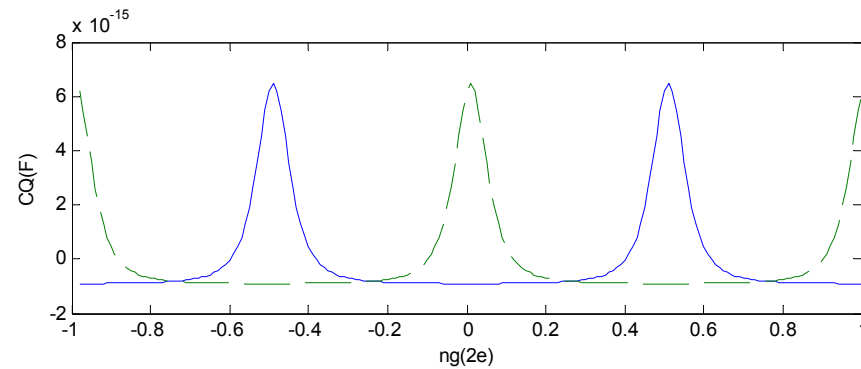
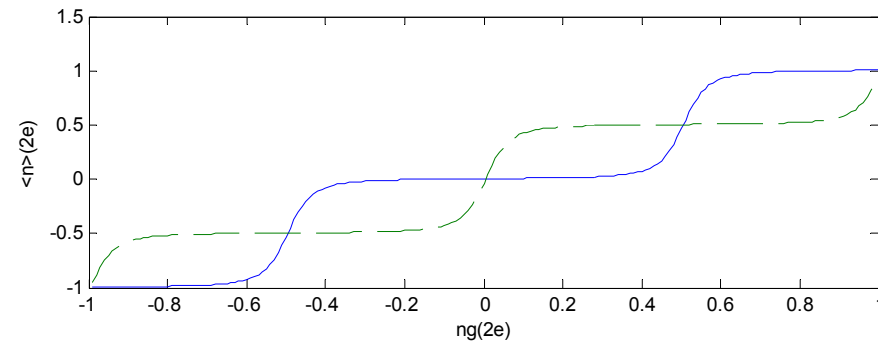
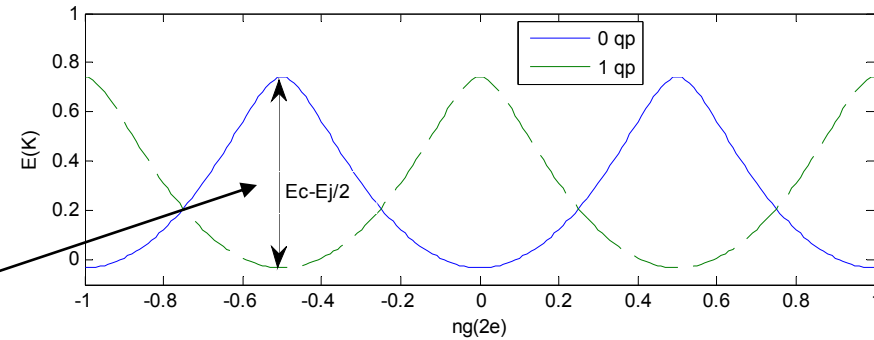




Quasiparticle Poisoning

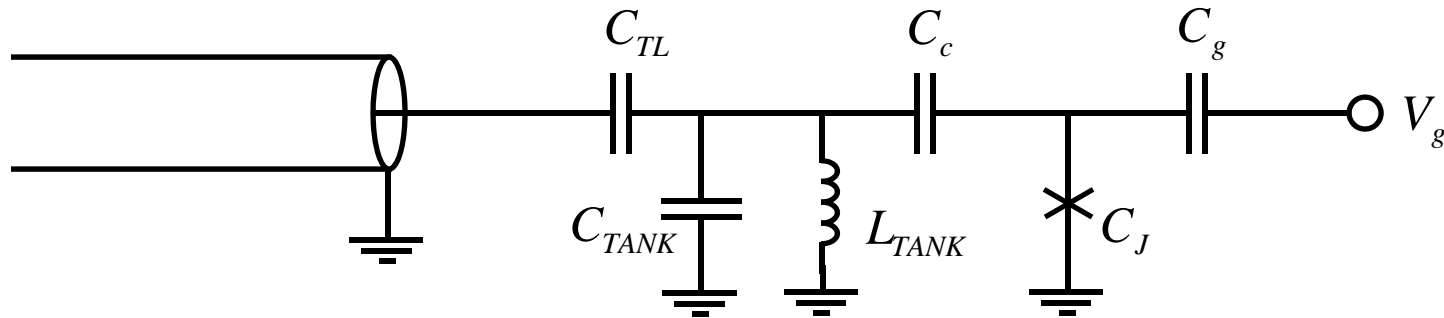


- If there are quasiparticles present in the leads, they could tunnel in and out of the island
- When they tunnel, they shift the effective gate voltage by e/C_g (or $n_g=0.5$)
- Coulomb staircase and quantum capacitance curve shifts by $n_g=0.5$ each time a quasiparticle tunnels in or out.





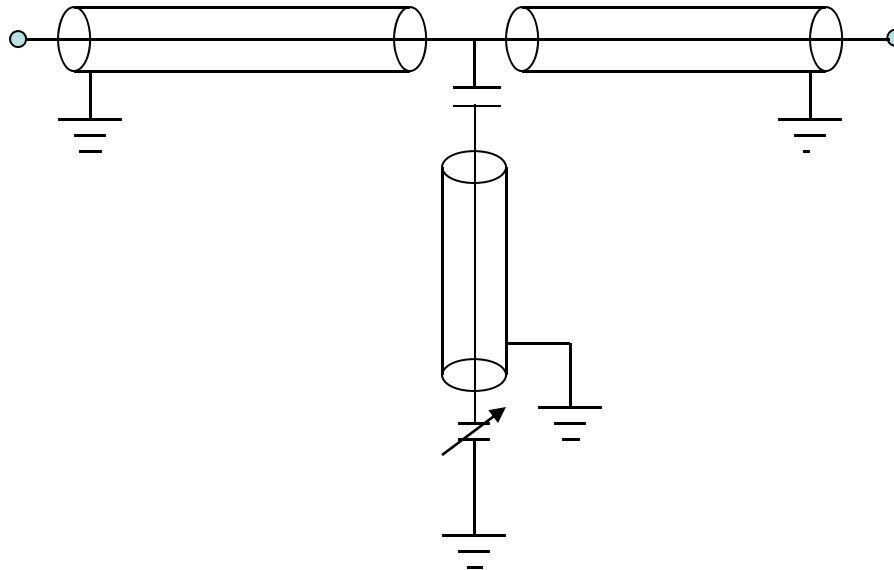
Measurement Technique



- Change in capacitance pulls the frequency of the oscillator
- Resonant frequency (~ 600 MHz) is far below qubit level spacing (~ 5 GHz)
- Noise and RF probe isolated from qubit
- Overall circuit capacitance is determined by qubit state
- Enables elegant multiplexing of many qubits
- Phase shift is measured with quadrature mixer



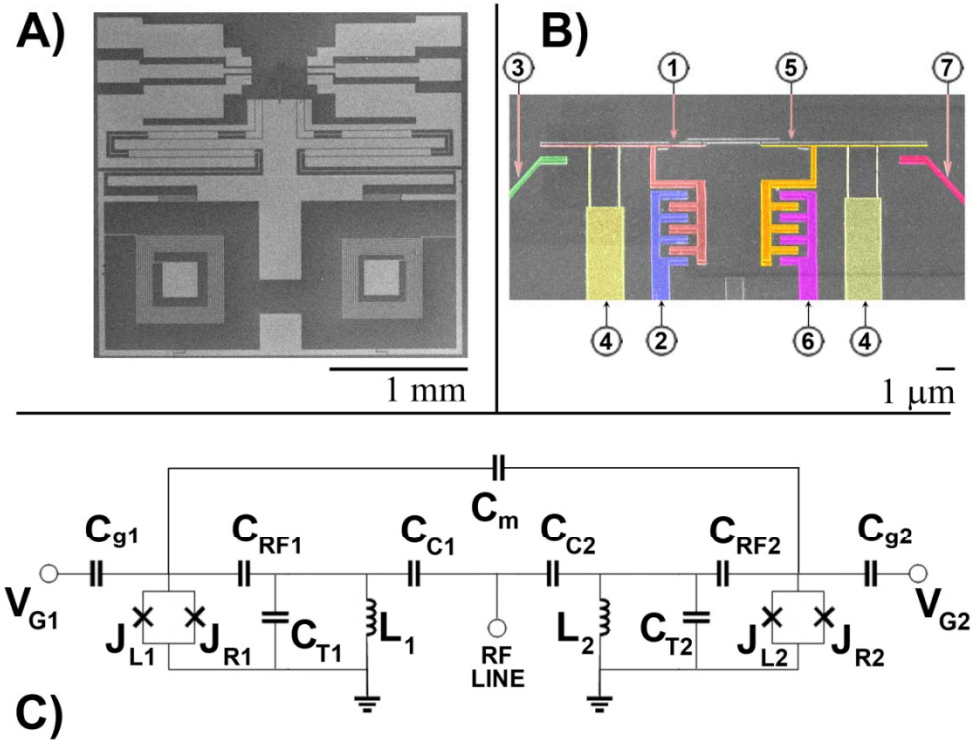
Measurement Technique



- In actual detectors we will use $\lambda/2$ resonator capacitively coupled to a feedline
- SCB is the variable capacitor at the end of resonator



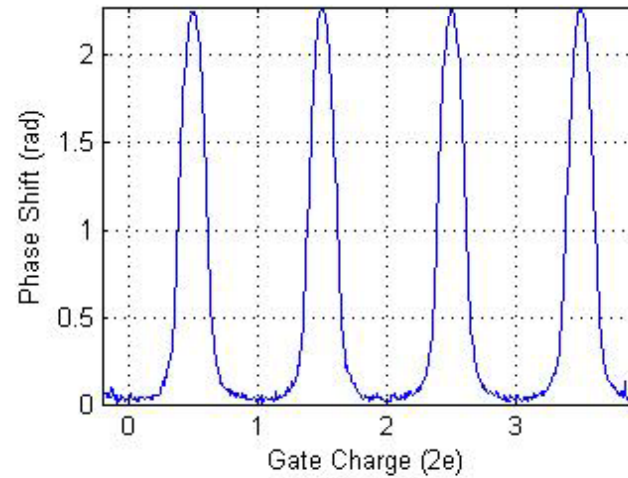
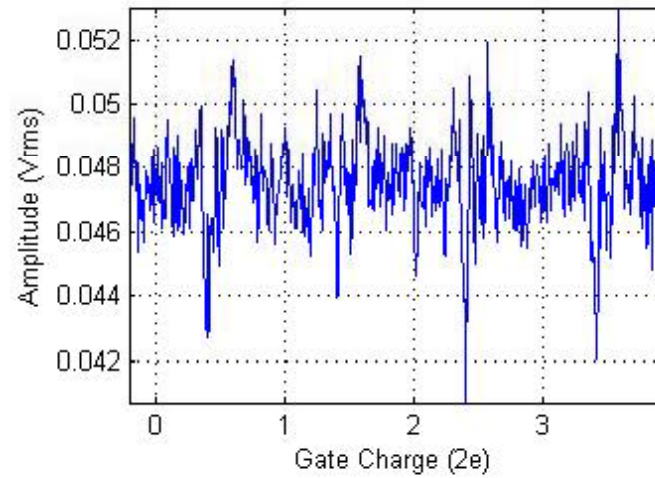
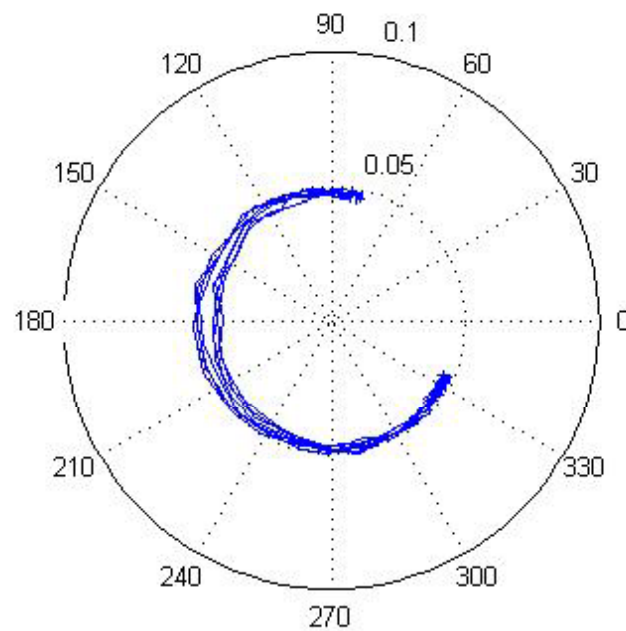
Experimental Setup



- Two SCBs with multiplexed quantum capacitance readout

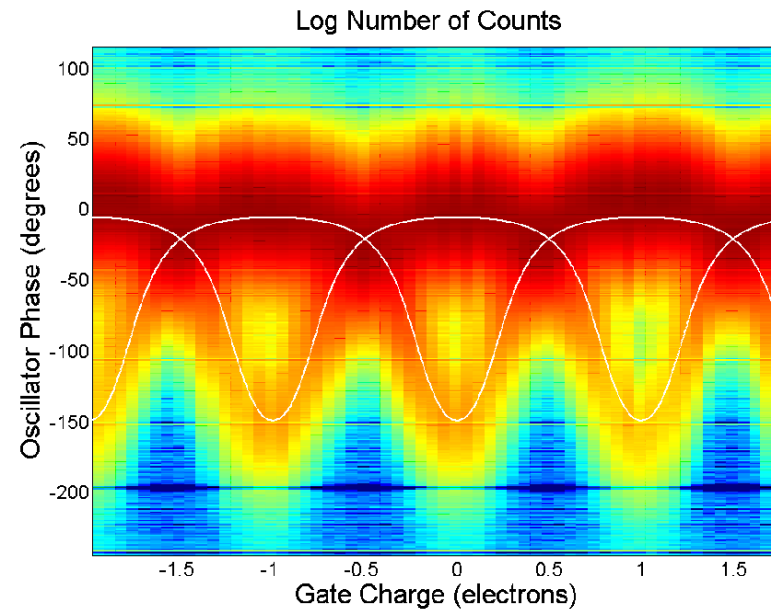
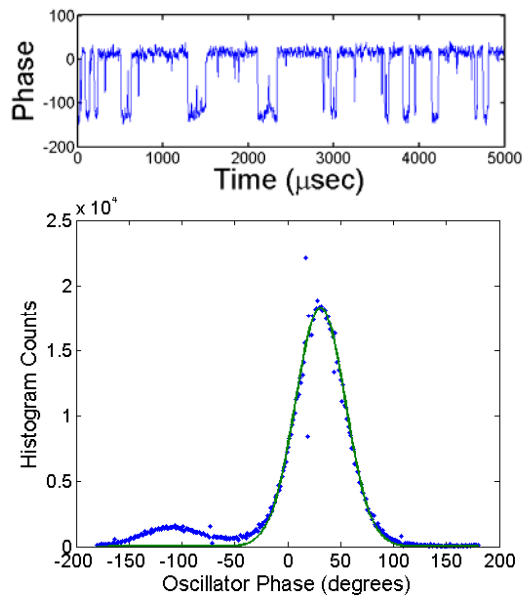


Experimental measurements





Tunnel Rate Measurements



- Phase measured at degeneracy point in real time
- One quasiparticle tunnel event shifts phase by ~ 140 degrees
- Can study statistics and compare with existing theory



Dependence on Quasiparticle Density

$$\Gamma_{in} \approx Kn_{qp} \quad \Gamma_{out} \text{ independent of } n_{qp}$$

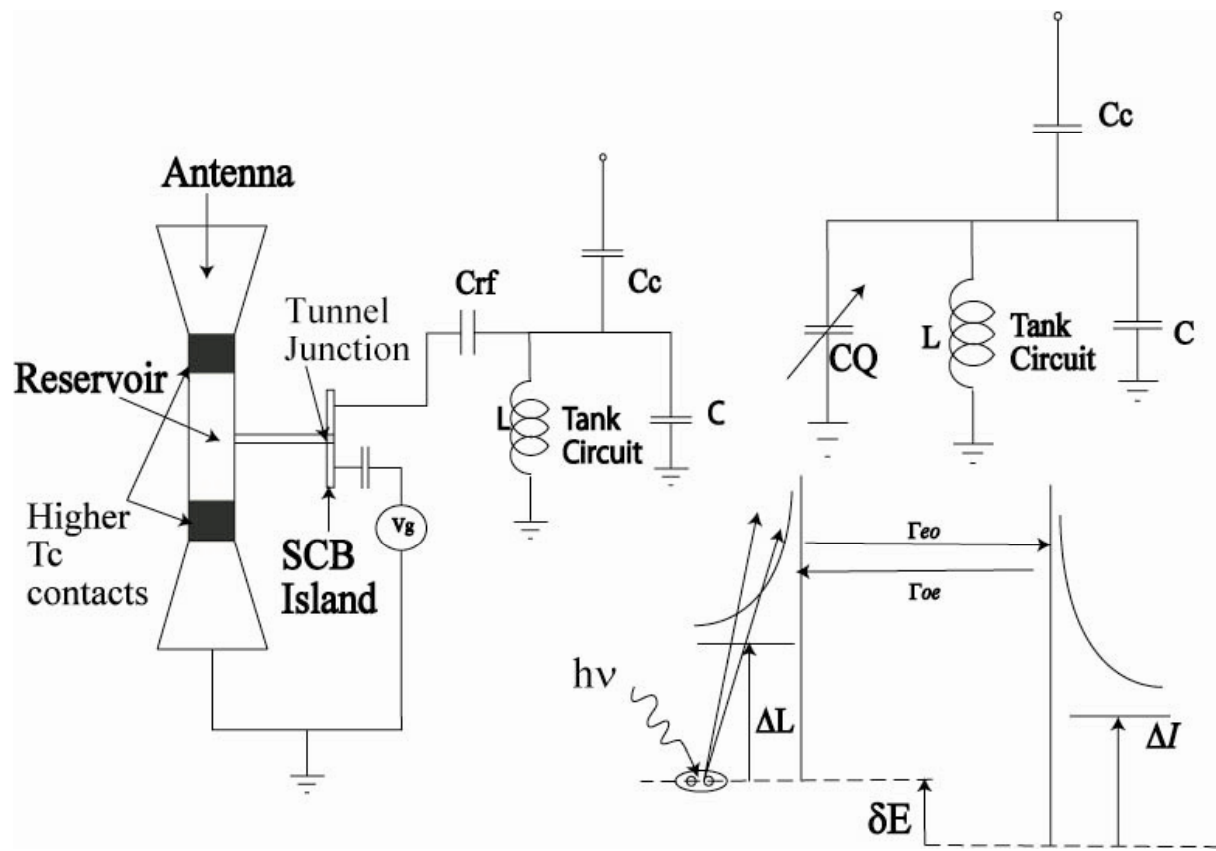
$$K = \frac{G_N}{e^2} \frac{e^{\Delta_L/kT}}{N_L} \int_{\max(\Delta_I - \delta E, \Delta_L)}^{\infty} dE \frac{E(E + \delta E) - \Delta_L \Delta_I}{\sqrt{((E + \delta E)^2 - \Delta_I^2)(E^2 - \Delta_L^2)}} e^{-E/kT}$$

- Approximations valid at low temperature
- Simple relationship between rates and QP density is ideal for detector

$$P_{odd} = \frac{\Gamma_{in}}{\Gamma_{in} + \Gamma_{out}}$$



The Quantum Capacitance Detector



- Radiation coupled by an antenna breaks Cooper pairs in the reservoir (absorber)
- Quasiparticles tunnel onto the island with a rate Γ_{in} proportional to the quasiparticle density in the reservoir
- Quasiparticles tunnel out of the island with a rate Γ_{out} independent of the number of quasiparticles in the reservoir
- At steady state the probability of a quasiparticle being present in the island is given by $Po(Nqp) = \Gamma_{in} / (\Gamma_{in} + \Gamma_{out})$
- The resulting change in the average capacitance will be $C_Q = (4E_C / E_J) (C_g^2 / C_s) Po(Nqp)$
- This change in capacitance will produce a phase shift $\delta\Phi \sim 2C_Q / (\omega_o Z_o C_c^2)$
- With the existing tank circuit parameters, phase shift per quasiparticle should be 138 degrees, in very good agreement with experiments



Noise Sources and NEP

- Phase noise – from phase measurement histogram the rms phase noise is ~ 33 degrees or 1.8×10^{-3} radian/Hz^{1/2} over the 100kHz bandwidth

- Telegraph noise: the tunneling on and off the island is approximated as a Poisson process with rates Γ_{eo} and Γ_{oe} . At low frequencies the spectral density of noise associated with the process is

$$S_{\Phi}^{Tele} = \frac{\delta\Phi^2}{\pi} \frac{\Gamma_{eo}\Gamma_{oe}}{(\Gamma_{eo} + \Gamma_{oe})^2}$$

- Fano noise: the number of quasiparticles generated by an incoming photon has an uncertainty given by $(FN_{qp})/2$ where $F \sim 0.2$ is the Fano factor for this system. The associated NEP is

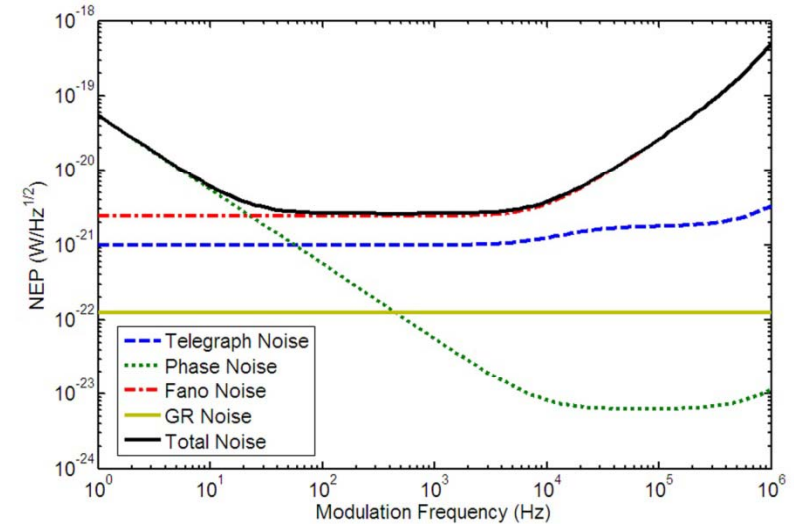
$$NEP^{Fano} = \sqrt{\frac{FP_S \Delta}{\eta}}$$

- Generation-recombination noise: quasiparticles can be thermally excited over the superconducting gap and recombine into Cooper pairs, introducing a fluctuation in the number of quasiparticles in the reservoir. The associated NEP is

$$NEP_{GR} = 2\Delta_L \sqrt{\frac{N_{eq}}{\tau_R}}$$

- The noise equivalent power at low frequencies will be given by

$$NEP = \sqrt{\left(\frac{dP_S}{dN_{qp}}\right)^2 \left(\frac{d\Phi}{dN_{qp}}\right)^{-2} (S_{\Phi}^{Phase} + S_{\Phi}^{Tele}) + NEP_{GR}^2 + NEP_{FANO}^2}$$



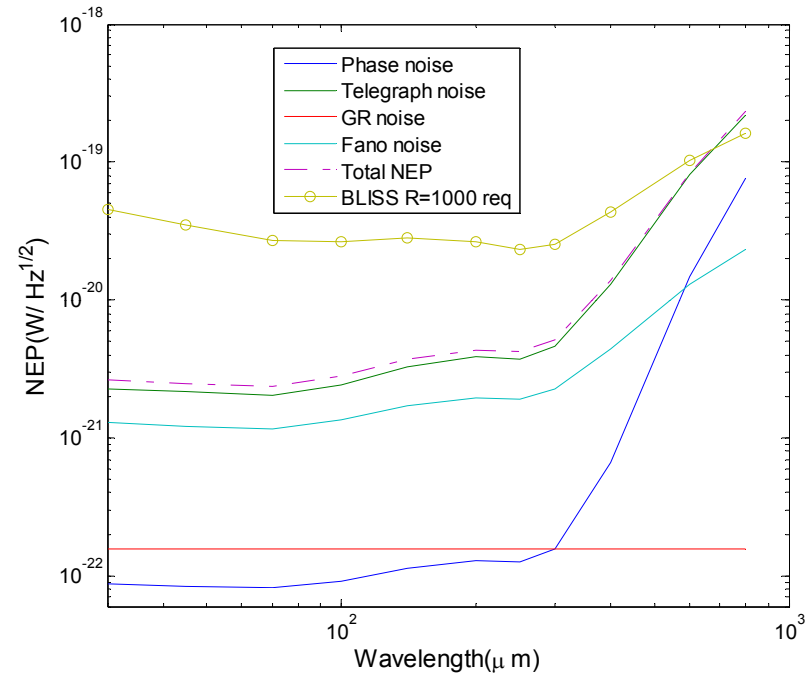
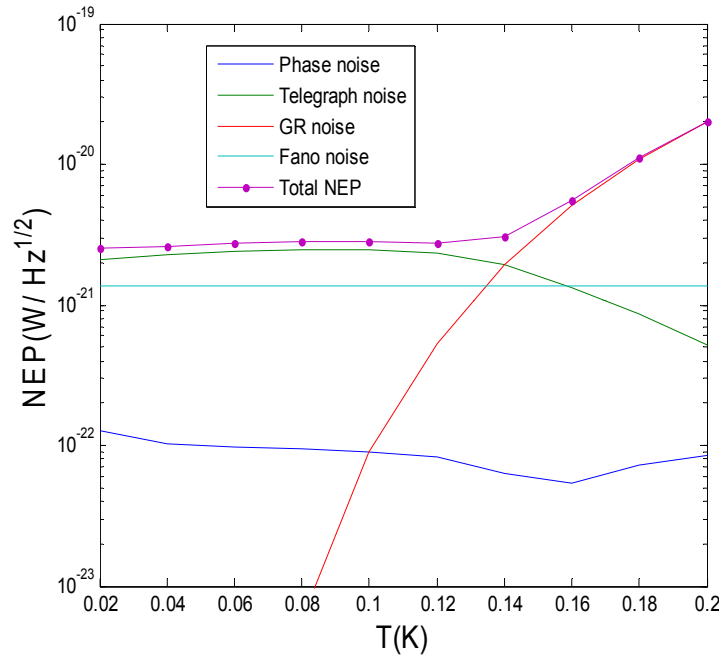
$$N_{qp} = \frac{\eta P_S \tau_{qp}}{\Delta} \quad \frac{d\phi}{dn_{qp}} = \frac{2C_Q}{\omega_o Z_o C_C^2} \frac{\Gamma_{out} K}{(Kn_{qp} + \Gamma_{out})^2}$$

N_{eq} is the number of equilibrium quasiparticles.

$$N_{eq} = \Omega_L D(E_F) \sqrt{\frac{\pi k_B T \Delta_L}{2}} \exp\left(-\frac{\Delta}{k_B T}\right)$$



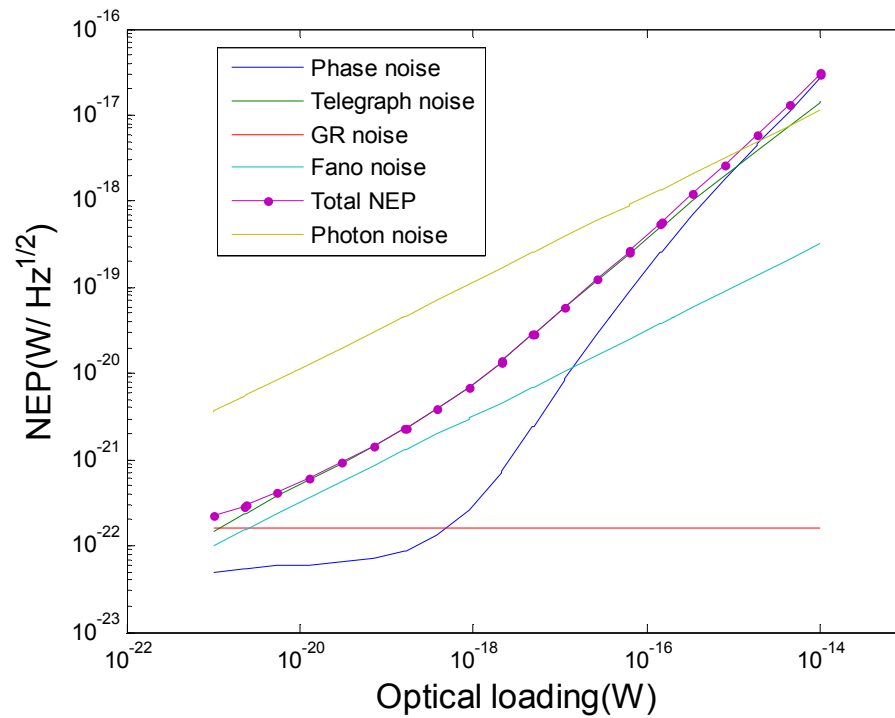
Theoretical Sensitivity



Left: NEPs from various noise sources calculated for devices optimized for $\lambda = 100\mu m$, optical loading 10^{-19} W and $R=1000$ as a function of temperature. Right: NEPs of various noise sources as a function of wavelength as compared to the requirements for a spectrometer with $R=1000$ and the expected optical loading at L2 for a cold (4.2K) telescope. The operating temperature was chosen to be 0.1K at which the GR noise contribution is negligible.



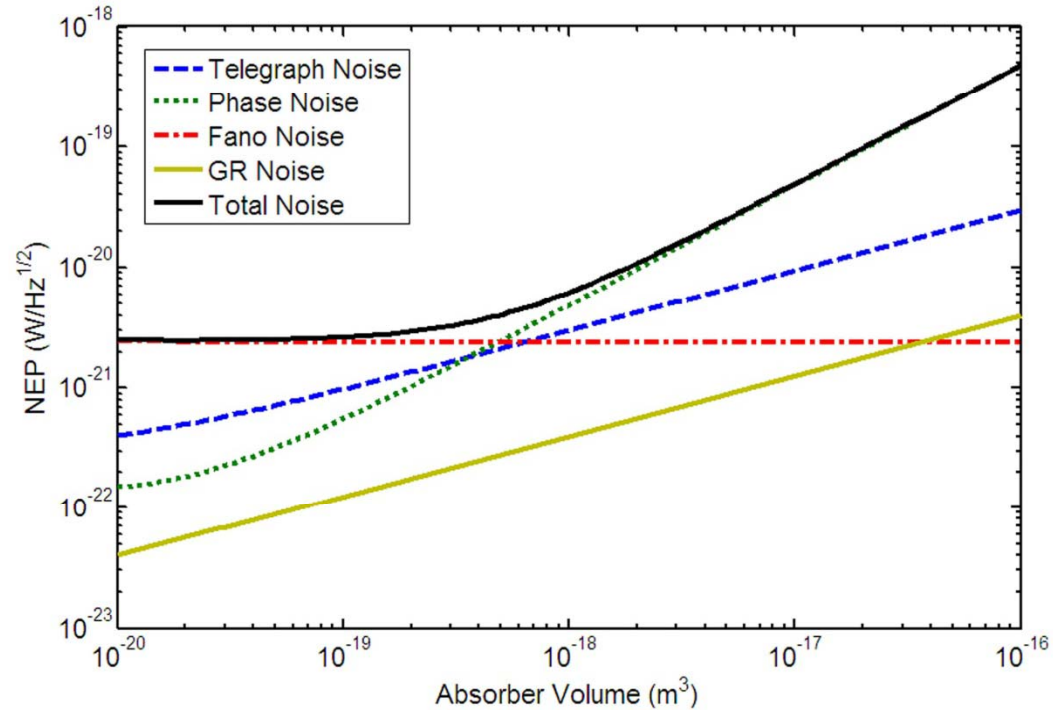
Theoretical Sensitivity vs. Signal Power



- *Detector is background limited over a wide range of operation*



Theoretical Sensitivity vs. Absorber Volume

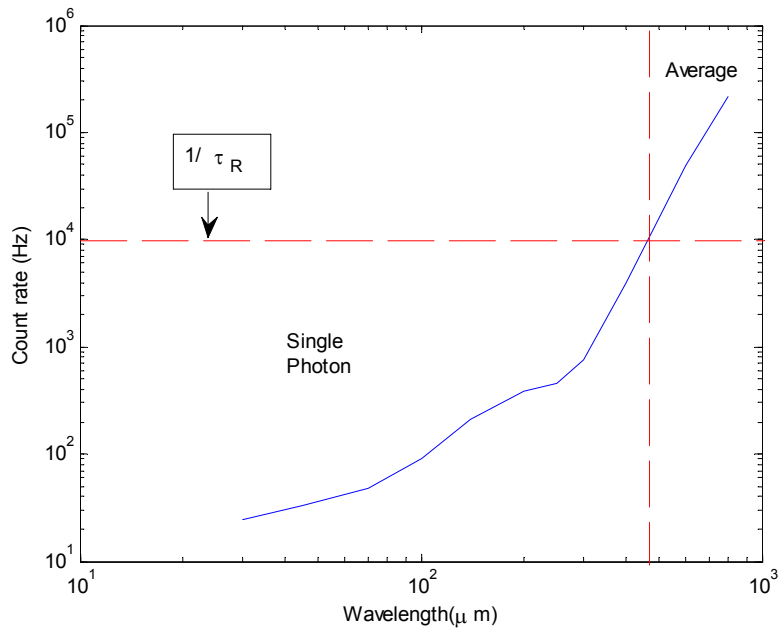


- Absorber volume is a key parameter
- Can be used to trade sensitivity for saturation power



Single Photon Detection

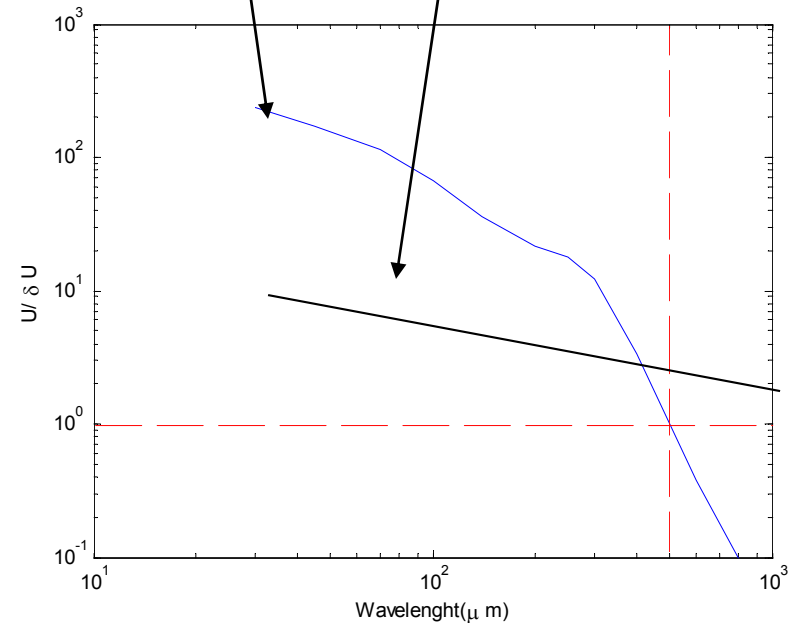
Photon arrival rate for a cold (4K) telescope with an R=1000 spectrometer at L2 as a function of wavelength



- From the NEP, the energy resolution will be

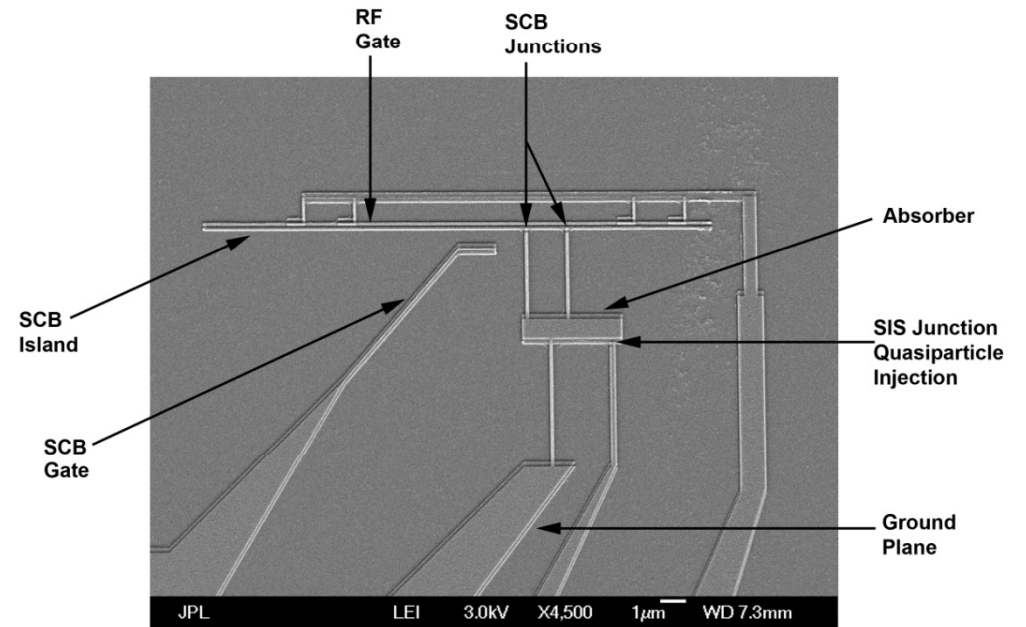
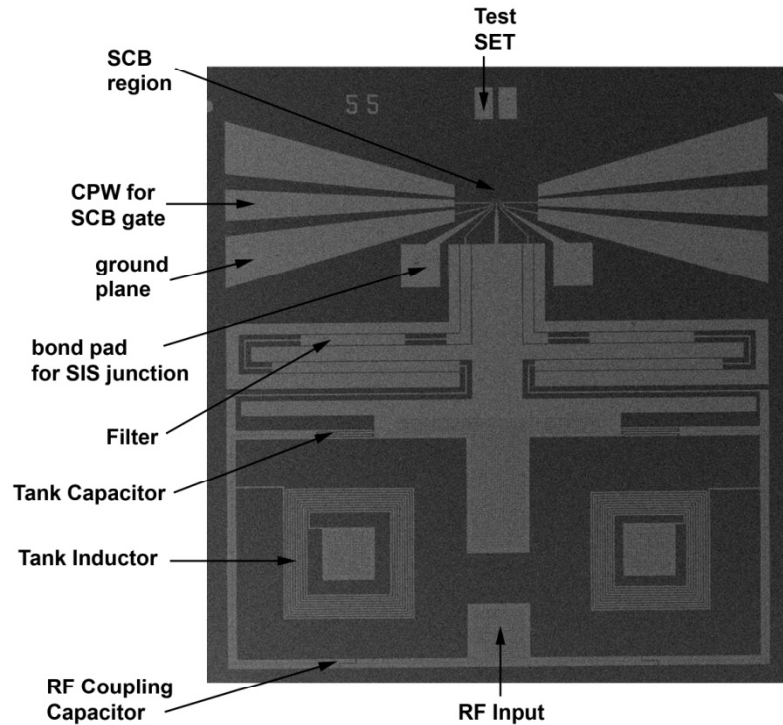
$$\delta U = NEP(0)\sqrt{\tau_R}$$

From Fano limit
$$\frac{U}{\delta U} = \frac{1}{2.36} \sqrt{\frac{\eta hc}{F\lambda\Delta}}$$



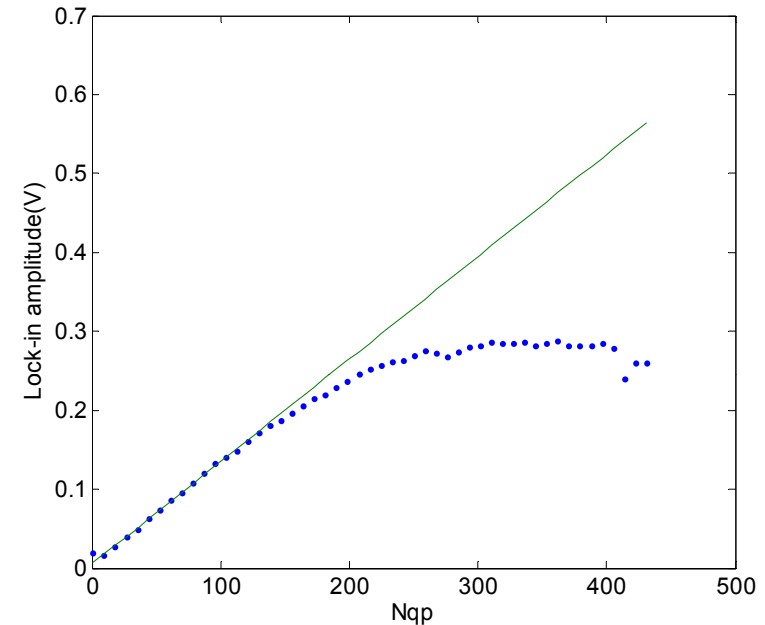
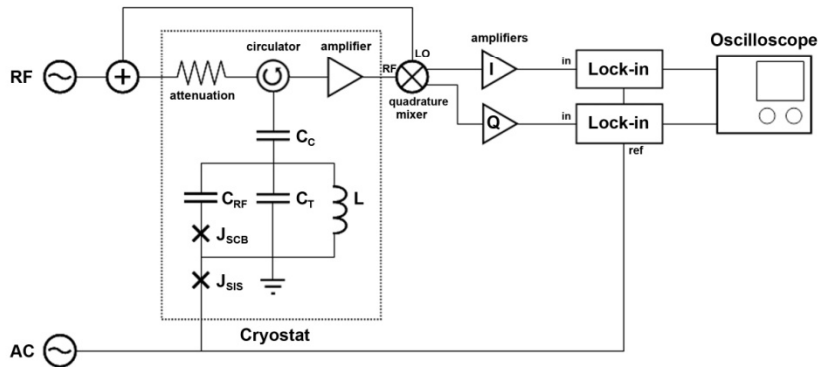


Experimental Confirmation Quasiparticle Injection with SIS junctions





Experimental demonstration Response versus signal



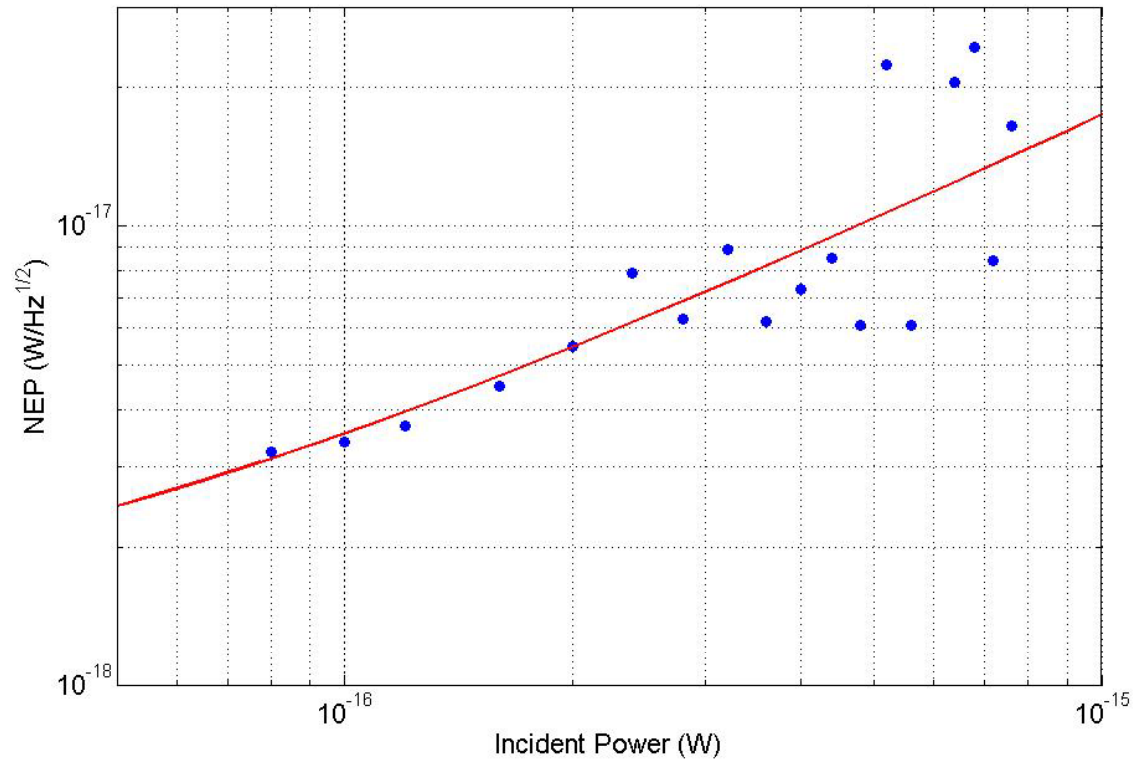
- Ran a current through SIS junction to inject quasiparticles on reservoir
- AC component of current simulates signal and DC optical loading
- τ_D is the time for quasiparticles to diffuse through constriction
- Graph shows lock-in response as a function of number of quasiparticles present in the reservoir.
- The measured noise in number of quasiparticles in the reservoir was $\delta N_{qp} \sim 11$ qp/Hz^{1/2}, which would yield an NEP $\sim 3 \times 10^{-18}$ W/Hz

$$N_{qp} = \frac{I}{e} \left(\frac{1}{\tau_R} + \frac{1}{\tau_D} \right)^{-1} \sim \frac{I}{e} \tau_D$$

$$NEP = \eta \frac{\Delta}{\tau_R} \delta N_{qp}$$

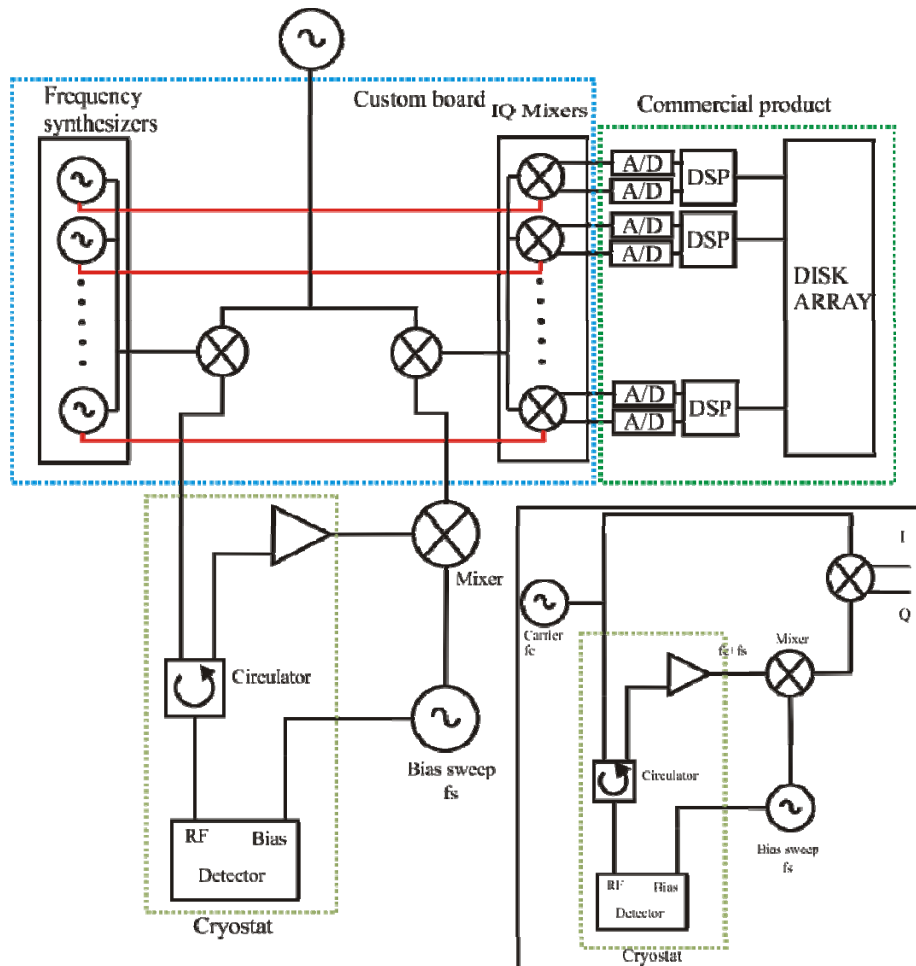


Experimental demonstration Response x loading





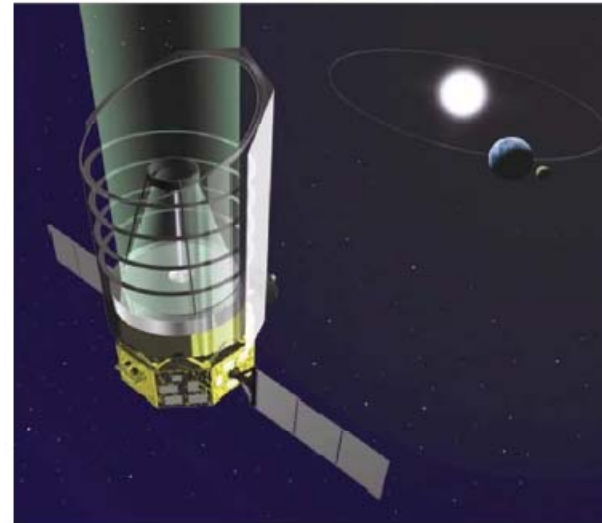
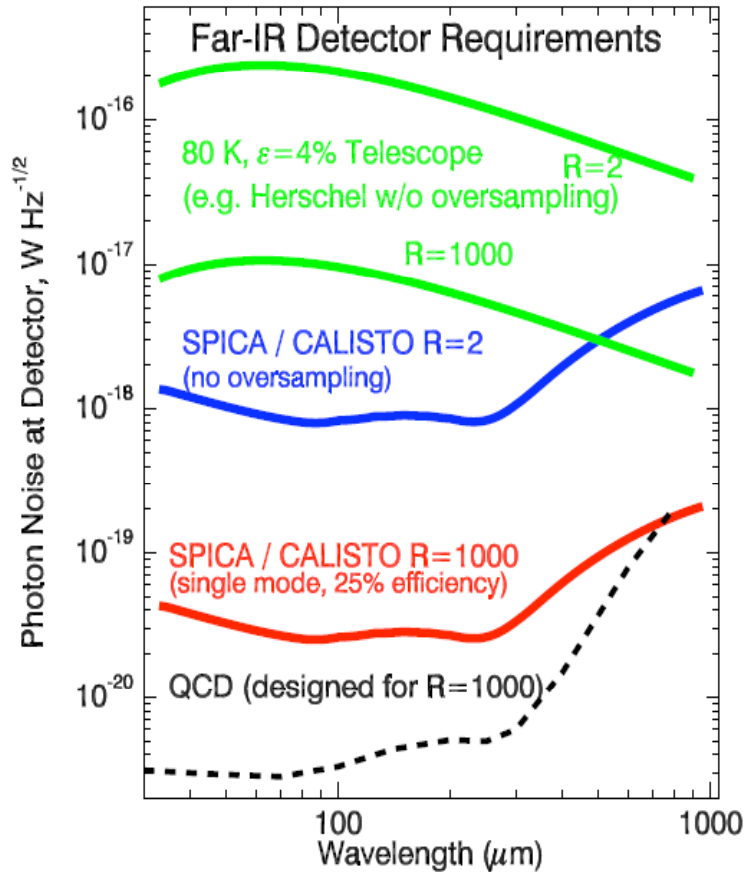
Multiplexing scheme



- Gates are swept with a low frequency f signal of amplitude e/Cg
- A mixer demodulates the reflected RF signal to the modulation frequency f and a down converter translates the results to DC
- In the multi-pixel readout, A low frequency comb function (0-200MHz) containing several frequency components is produced digitally using a D/A converter and then block up-converted, resulting in a comb of RF carrier frequencies with each frequency corresponding to a particular detector.
- All of the SCB gates are tied together through a common bias line and modulated at the same frequency.
- The reflected RF comb, containing the phase shift information for the entire array, is demodulated at the bias modulation frequency, down-converted to the 0-200MHz band, then digitized and digitally demultiplexed.



Applications in FIR-Submillimeter Astronomy



- Cold (4.2K) telescope at L2 with $R=1000$ spectrometer



Detector Advantages

- *SCB has extreme sensitivity to the presence of quasiparticles*
- *Sensitivity of QCD rivals MKID and TES*
- *Frequency-domain multiplexing allows scaling to large arrays*
- *Applicable to submillimeter wavelengths for far-infrared astrophysics*
- *Can be easily incorporated with existing technology for MKID arrays*
- *Detector (SCB) is separate from resonator – flexibility of design*
- *NEP and saturation power easily tailorable*